forests

MDPI

Article

Predicting the Potential Suitable Distribution of *Larix principis-rupprechtii* Mayr under Climate Change Scenarios

Ruiming Cheng, Xinyue Wang, Jing Zhang, Jinman Zhao, Zhaoxuan Ge and Zhidong Zhang *

College of Forestry, Hebei Agricultural University, Baoding 071000, China
* Correspondence: zhzhido@163.com

Abstract: *Larix principis-rupprechtii* Mayr (larch) is a native conifer species in North China, and also a major silvicultural and timber species in the region. Climate change has led to a change in its suitable distribution area. However, the dominant factors affecting changes in its suitable distribution and migration trends are not clear. In this study, based on forest resource inventory data and bioclimatic data in Hebei and Shanxi provinces, China, we built an ensemble model based on seven algorithms to simulate the larch's potential suitable distribution areas under three shared socioeconomic pathways (SSPs: SSP1-2.6, SSP2-4.5, and SSP5-8.5) for the current and future (2021–2040, 2041–2060 and 2080–2100). The results revealed that: (1) ensemble models significantly improved the predictive accuracy (ROC = 0.95, TSS = 0.81, KAPPA = 0.65); (2) the current potentially suitable distribution area was concentrated in the Bashang Plateau and the northwestern mountain range of the study area. Among them, 12.38% were highly suitable distribution areas, 12.67% were moderately suitable distribution areas, and 12.01% were lowly suitable distribution areas; (3) the main climatic factors affecting larch distribution were mean temperature of driest quarter, mean diurnal range, precipitation of warmest quarter, and temperature annual range; (4) under different future climate scenarios, the contraction of the suitable distribution area of larch increased significantly with increasing SSP radiation intensity. By 2100, the suitable distribution area of larch was expected to decrease by 26.5% under SSP1-2.6, 57.9% under SSP2-4.5, and 75.7% under SSP5-8.5 scenarios; (5) from 2021 to 2100, the different suitable distribution areas of larch showed a trend of migration to the northeast. Under the SSP5-8.5 scenario, the migration distance of different suitable distribution areas was the largest, in which the high suitable distribution area migrated 232.60 km, the middle suitable distribution area migrated 206.75 km, and the low suitable distribution area migrated 163.43 km. The results revealed the impact of climate change on the larch distribution, which provided a scientific basis for making forest management decisions.

Keywords: *Larix principis-rupprechtii*; ensemble model; climate change; suitable distribution; species distribution models

Citation: Cheng, R.; Wang, X.; Zhang, J.; Zhao, J.; Ge, Z.; Zhang, Z. Predicting the Potential Suitable Distribution of *Larix principis-rupprechtii* Mayr under Climate Change Scenarios. *Forests* **2022**, *13*, 1428. https://doi.org/10.3390/f13091428

Academic Editor: Mark Vanderwel

Received: 4 August 2022
Accepted: 1 September 2022
Published: 5 September 2022

1. Introduction

Climate change greatly affects the distribution of species [1] and is considered to be one of the major threats to biodiversity [2,3]. Forests play a key role in mitigating global warming [4,5]. In the context of global climate change, most tree species occupy a certain climatic niche [6] that is constantly changing. The consequence is that the habitat quality of species is degraded, the area is reduced, and species are forced to spread to polar regions or high elevations [7]. Due to the long growth cycle and slow migration of trees, it is difficult to adapt to rapidly changing climatic conditions [8]. According to the sixth assessment report of IPCC, climate change will be more severe in the future [9]. Therefore, in the context of continuous global warming, elucidating the change in tree distribution and the mechanism leading to this change has become the focus of the current research [10,11].

Inner Asian forests are sensitive to changes in temperature and precipitation [12,13]. In the past few decades, a significant rise in temperature in northern China has led to

severe drought [14]. Drought caused a large area of forest contraction [15] and massive death of trees [16]. It has also been suggested that future temperature increases will cause trees to migrate to higher elevations and higher latitudes [17–19]. The migration of trees to more suitable habitats is an adaptive response to climate change [20]. However, different tree species in different regions are not consistent in response to climate change, which brings challenges for forestry workers to formulate corresponding strategies [21]. Accurate determination of the impact of climate change on changes in trees' distribution is essential for forest management [22]. Shared socioeconomic pathways (SSPs) have high climate sensitivity in the context of global warming and the consequent climatic changes [9]. Among them, four core scenarios were widely used in research on species distribution, namely, SSP1-2.6, SSP2-4.5, SSP3-7.0, and SSP5-8.5.

Species distribution models (SDMs) are effective tools to predict the geographical range of species by combining environmental variables and species location information [23]. With the development of remote sensing and geographic information technology, SDMs are widely used in biodiversity assessment [24], species potential distribution prediction [25], protection of rare species [26,27], and so on. At present, the widely used SDMs include random forest (RF) [6], artificial neural network (ANN) [28], generalized linear model (GLM) [29], maximum entropy (MaxEnt) [30], etc. However, because the principles and algorithms of each model are different, it is difficult to select an appropriate model to predict precisely the suitable distribution of species [31]. In order to solve this kind of uncertainty, more and more research has adopted the ensemble modeling approach, which combines predictions across different modeling methods [32]. The ensemble model (EM) is considered to be an effective method to evaluate the potential distribution of species at a large spatial scale [33], and can effectively solve the uncertainty caused by a single model [34]. The EM has been used to predict the distribution of forests [35,36] and other species [37], and good prediction accuracy has been obtained.

Larch forest plays a key role in the regional carbon budget [38,39], and larch is one of the most sensitive tree species to climate change [40]. The study indicates that the future distribution of *Larix chinensis* Beissn. in the low-altitude areas of the Qinling Mountains will become extinct, and the suitable habitat will be transferred to higher-altitude areas [1]. In China, the suitable distribution area of *L. kaempferi* (Lamb.) Carr. will be reduced and migrated northward [41]. Larch species distributed in Northeast China show different migration patterns and respond to climate change by reducing and expanding the suitable distribution area [42,43]. *L. principis-rupprechtii* is one of the commonly used afforestation tree species in North China [44], which has high economic and ecological value [45]. The suitable distribution pattern of *L. principis-rupprechtii* has changed under the influence of dominant climate factors [46,47]. However, most of the previous studies are based on a single model, and there is a lot of uncertainty in the results. Therefore, the EM is used to predict the suitable distribution of *L. principis-rupprechtii*, which is intended to improve the prediction accuracy and provide a reference for planting area management.

In this study, we selected *L. principis-rupprechtii*, which is widely distributed in Hebei and Shanxi provinces, as the research object, and used the EM to predict its potential distribution under baseline and different projected future climate change scenarios. The research mainly solves the following three problems: (1) is there any change in the potential suitable distribution area at current and projected future climate change scenarios; (2) what are the main climatic factors affecting the potential distribution of *L. principis-rupprechtii*; (3) whether the migration trend of suitable distribution areas is consistent in different periods and climatic scenarios. The results of this study can provide a theoretical basis for the adaptive management of *L. principis-rupprechtii*.

2. Materials and Methods

2.1. Study Area

Hebei and Shanxi provinces (110°14–119°50 E, 34°34–42°40 N) are the primary distribution areas of *L. principis-rupprechtii* in China. The terrain of the region is characterized by

complex and diverse types of landforms, including plateaus, mountains, hills, and basins. The average elevation in the mountains is around 1500 m. The study area is characterized by a temperate continental monsoon climate with a hot and rainy summer and a cold and dry winter. The annual temperature is 4–14 °C, and the annual precipitation is 300–800 mm [48,49]. The dominant species include *L. principis-rupprechtii*, *Pinus tabulaeformis* Carr., *Platycladus orientalis* (Linn.) Franco, *Quercus mongolica* Fisch. ex Ledeb. etc. [50].

2.2. Species Occurrence Data

The geographical occurrence data for *L. principis-rupprechtii* were from a variety of sources, including forest resources inventory data in Hebei Province and Shanxi Province, field survey data (temporary and permanent sampling plots), the Chinese Virtual Herbarium (http://www.cvh.ac.cn (accessed on 15 November 2021))and the National Specimen Information Infrastructure (http://www.nsii.org.cn (accessed on 15 November 2021)). To improve the predictive accuracy, we selected only occurrence data points with natural origin. In addition, to avoid overrepresentation of climatic conditions in densely sampled areas and prevent spatial autocorrelation, a minimum distance of 3 km between sampling points was considered. Finally, we obtained a total of 306 distribution points to build the model (Figure 1).

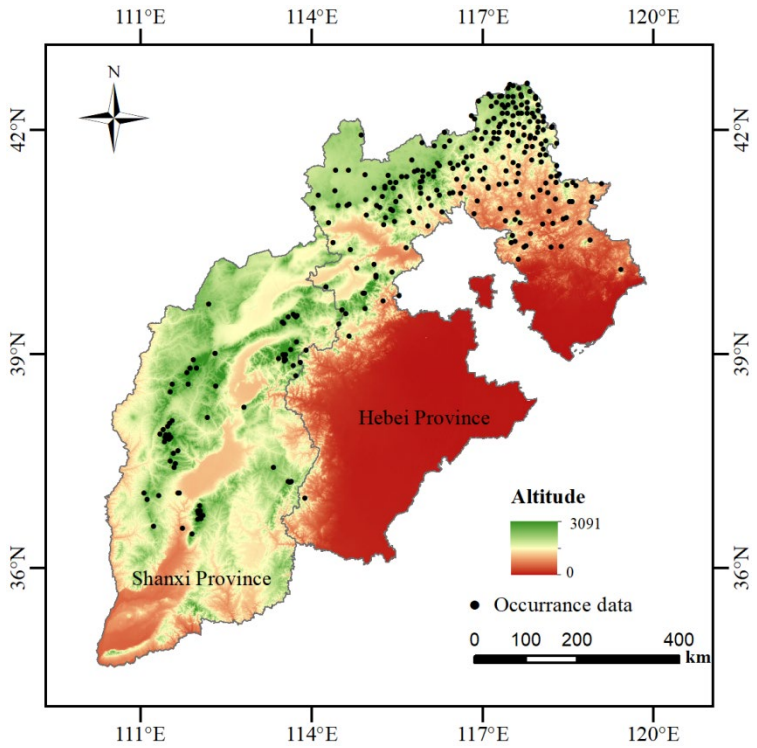

Figure 1. Study area and geographic locations of *Larix principis-rupprechtii* population distribution.

2.3. Environmental Variables

The current and future (2021–2100) bioclimatic data with a 30 arc-second resolution (approximately 800 m) were obtained from the WorldClim database (http://www.Worldclim.org (accessed on 18 November 2021). We selected medium-resolution Beijing Climate Center Climate System Model version 2 (BCC-CSM2-MR), which is widely used in China, to derive future climate change scenario data. Three future climate scenarios, including low radiation intensity (SSP1-2.6), medium radiation intensity (SSP2-4.5), and high radiation intensity (SSP5-8.5) were used. We also simulated the suitable distribution of larch species in three future periods: 2030s (average for 2021–2040), 2050s (average for 2041–2060), and 2090s (average for 2081–2100) under the projected climate change scenarios mentioned above [51]. Study shows that a 10-fold change in resolution will not seriously affect the

fitting accuracy of the species distribution model [23]. Considering comprehensively, a total of 19 climatic factors related to temperature and precipitation were resampled at 250 m resolution.

In order to avoid the problem of model fitting due to the collinearity of climatic factors [52], correlation analysis and variance inflation factor analysis [53,54] were carried out. Climatic factors with $|r| < 0.8$ and VIF < 10 were selected. Finally, eight climatic factors were selected to build the model (Table 1).

Table 1. Climatic factors used to predict the potential distribution of larch. The variables selected for building model are marked with an asterisk (*).

Variable Name	Code	Unit	VIF
Annual mean temperature	BIO1	°C	
Mean diurnal range (mean of monthly (max temp—min temp))	BIO2 *	°C	2.87
Isothermally (BIO2/BIO7) (* 100)	BIO3 *	-	3.71
Temperature seasonality (standard deviation * 100)	BIO4	-	
Max temperature of warmest month	BIO5 *	°C	1.71
Min temperature of coldest month	BIO6	°C	
Temperature annual range (BIO5-BIO6)	BIO7 *	°C	5.46
Mean temperature of wettest quarter	BIO8	°C	
Mean temperature of driest quarter	BIO9 *	°C	3.77
Mean temperature of warmest quarter	BIO10	°C	
Mean temperature of coldest quarter	BIO11	°C	
Annual precipitation	BIO12	mm	
Precipitation of wettest month	BIO13	mm	
Precipitation of driest month	BIO14	mm	
Precipitation seasonality (coefficient of variation)	BIO15 *	mm	7.69
Precipitation of wettest quarter	BIO16	mm	
Precipitation of driest quarter	BIO17	mm	
Precipitation of warmest quarter	BIO18 *	mm	4.57
Precipitation of coldest quarter	BIO19 *	mm	1.87

2.4. Research Methods

2.4.1. Establishment of Single Species Distribution Model

This study used 10 model algorithms in the "biomod2" package in R 3.6.3 [34,55,56]. These model algorithms included surface range envelope (SRE), flexible discriminant analysis (FDA), classification tree analysis (CTA), generalized boosting model (GBM), ANN, RF, MaxEnt, GLM, generalized additive model (GAM), and multiple adaptive regression splines (MARS). Most SDMs require species absence data. In this research, we randomly generated pseudo-existence point data at least 3 km between the pseudo-existence points and the existence point data [27,32]. To reduce the predictive uncertainty caused by the randomly generated point position, we generated three sets of pseudo-absence data, and the number of pseudo-existence points in each group was 1500. The sample data (including occurrence data and pseudo sampling points) were randomly divided into two parts: 75% of the data as the training data set, and 25% as the test data set [27]. Each model algorithm was repeated 10 times with every sample dataset. A total of 300 single model results were obtained (3 sets of sample data × 10 model algorithms × 10 replicates). For all modeling algorithms, we used the default setting of the "biomod2" package [57].

2.4.2. Model Evaluation

We choose three kinds of model evaluation metrics embedded in the "biomod2" package to evaluate the fitting accuracy. Cohen's kappa statistic (KAPPA) was used to evaluate the consistency between sample data and simulation results. The true skill statistic (TSS) developed from KAPPA contained the advantages of KAPPA while avoiding its disadvantages. Receiver operating characteristic (ROC) was the most widely used index to evaluate the model. The area under ROC curve (AUC) value could indicate the accuracy of

the model prediction. The higher the value, the stronger the prediction ability of the model. The reference criteria for the three evaluation indicators are shown in Table 2 [58–60].

Table 2. Model evaluation index reference standard.

Evaluation Index	Excellent	Better	Moderate	General	Failure
Kappa	0.80–1.00	0.60–0.80	0.40–0.60	0.20–0.40	0.00–0.20
TSS	0.80–1.00	0.60–0.85	0.40–0.60	0.20–0.40	0.00–0.20
ROC	0.90–1.00	0.80–0.90	0.70–0.80	0.60–0.70	0.00–0.60

2.4.3. Ensemble Model Construction

To reduce the uncertainty caused by modeling algorithms, we comprehensively considered the two evaluation indicators of ROC and TSS to build the EM [53]. Only single model results with an ROC value greater than 0.9 and TSS value greater than 0.7 were retained, and the EM was constructed by the weighted average method. The results were projected on the ArcGIS 10.2 platform. The distribution areas of *L. principis-rupprechtii* were divided into four classes [53]: unsuitable area (0.0–0.2), lowly suitable area (0.2–0.4), moderately suitable area (0.4–0.6), and highly suitable area (0.6–1.0). At the same time, we overlaid suitable and unsuitable area classifications under current and future climate scenarios, and finally obtained the unsuitable areas, unchangeable potential suitable areas, degraded potential suitable areas, and increased potential suitable areas under future climate scenarios [32].

2.4.4. Dominant Environmental Factor Analysis

The relative importance of the environmental factors was assessed using the biomod2 method. Pearson's correlation coefficient between the reference prediction and the "shuffled" prediction was also calculated. The important value of each variable was 1 minus the correlation coefficient. The higher the score was, the more important the variable was [53,56]. In this study, the relative importance percentage of environmental factors in the final model was obtained by calculating the average value of different environmental factors through multiple operations. Finally, the response curves were used to analyze the dominant factors affecting the suitable distribution of *L. principis-rupprechtii* based on the results of the optimal model.

2.4.5. Centroid Shifts

We used the ArcGIS10.2 platform to calculate the area of highly suitable areas, moderately suitable areas, and lowly suitable areas under different climate scenarios for the current and future respectively. In addition, we used the SDM toolbox [61] to calculate the location of centroids in different periods and draw shift paths under different climatic scenarios [2,53].

3. Results

3.1. Model Accuracy Evaluation

Based on the values of ROC, KAPPA, and TSS metrics (Figure 2), the predictive performance of the SRE algorithm was proved the worst. The algorithms with a mean ROC value greater than 0.9, a mean TSS value greater than 0.7, and a mean KAPPA value greater than 0.52 were selected for ensemble modeling. Finally, seven algorithms were selected (FDA, GBM, RF, MAXENT, GLM, ANN, and MARS). The ROC, TSS, and KAPPA values of the EM were 0.95, 0.81, and 0.65, respectively, indicating more accurate predictions than all of the single models.

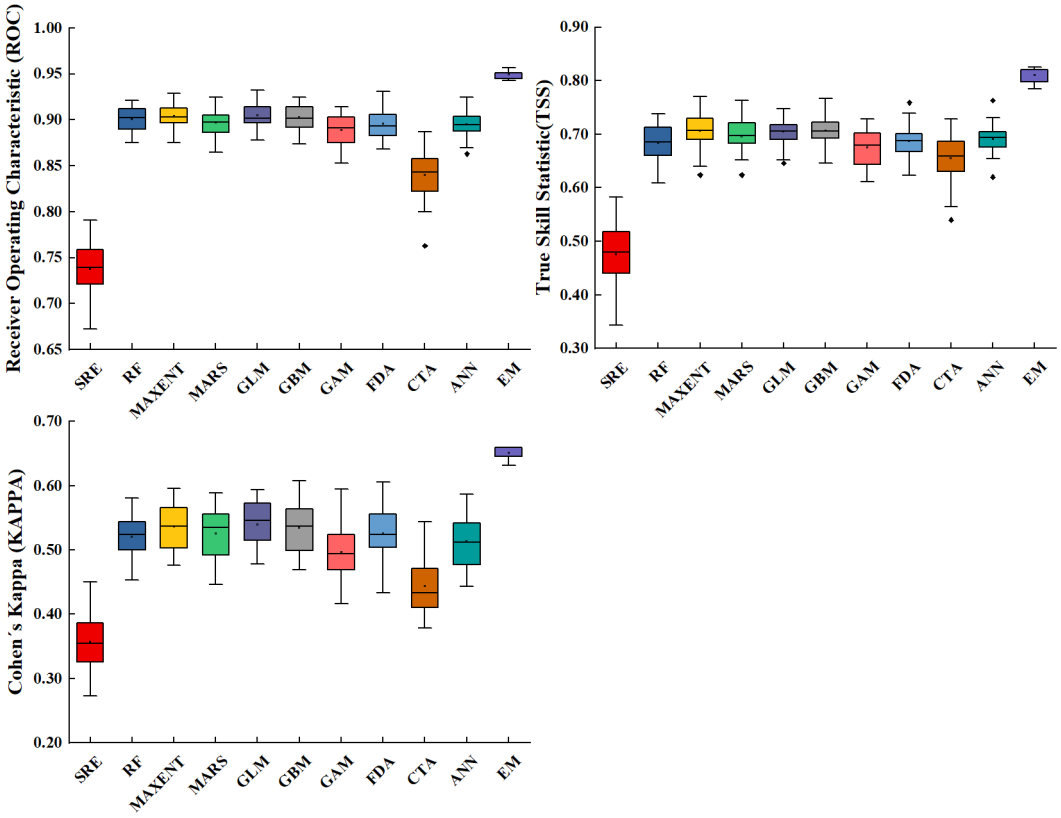

Figure 2. Comparison of ROC, TSS and KAPPA of ten models and ensemble model. MARS: multiple adaptive regression splines; GLM: generalized linear model; GBM: generalized boosting model; CTA: classification tree analysis; ANN: artificial neural network; SRE: surface range envelope; FDA: flexible discriminant analysis; RF: random forest; GAM: generalized additive model; MAXENT: maximum entropy. Black diamond blocks represent outliers.

3.2. Importance of Environmental Factors

The results of the relative importance analysis of climatic factors showed that the cumulative contribution rate of mean temperature of driest quarter (BIO9), mean diurnal range (BIO2), precipitation of warmest quarter (BIO18), and temperature annual range (BIO7) was 81.25%, indicating that the four climatic factors were the main factors affecting the larch suitable distribution (Table 3).

Table 3. Variable contribution (%) in different models. MARS: multiple adaptive regression splines; GLM: generalized linear model; GBM: generalized boosting model; CTA: classification tree analysis; ANN: artificial neural network; SRE: surface range envelope; FDA: flexible discriminant analysis; RF: random forest; GAM: generalized additive model; MAXENT: maximum entropy.

Variable	MARS	GLM	GBM	CTA	ANN	SRE	FDA	RF	GAM	MAXENT	Relative Importance
BIO9	62.59	58.09	76.28	72.99	37.40	25.82	48.25	40.02	32.44	79.00	53.29
BIO2	12.87	14.38	5.18	11.84	9.39	15.94	12.02	7.16	18.01	5.48	11.23
BIO18	7.94	7.23	11.39	9.72	14.22	9.94	9.07	10.80	5.18	9.53	9.50
BIO7	6.82	12.25	0.18	0.00	9.92	3.93	12.07	9.17	17.64	0.29	7.23
BIO5	0.92	1.26	3.56	1.15	6.34	19.54	6.94	16.67	5.43	2.39	6.42
BIO3	7.20	5.77	3.11	3.12	2.33	8.75	8.48	7.74	16.00	1.16	6.37
BIO15	1.19	0.61	0.30	1.18	11.72	13.12	1.38	6.53	4.53	1.54	4.21
BIO19	0.47	0.41	0.01	0.00	8.68	2.97	1.78	1.92	0.77	0.60	1.76

Response curve analysis showed that the occurrence probability of larch decreased with increasing BIO9. The higher suitability for larch occurred in areas with BIO2 less than

13.5 °C. The occurrence probability increased with increasing BIO18, and the occurrence probability reached the maximum value when the precipitation reached 405 mm. Larch showed a higher suitability in areas with a BIO7 of 27–48.3 °C (Figure 3).

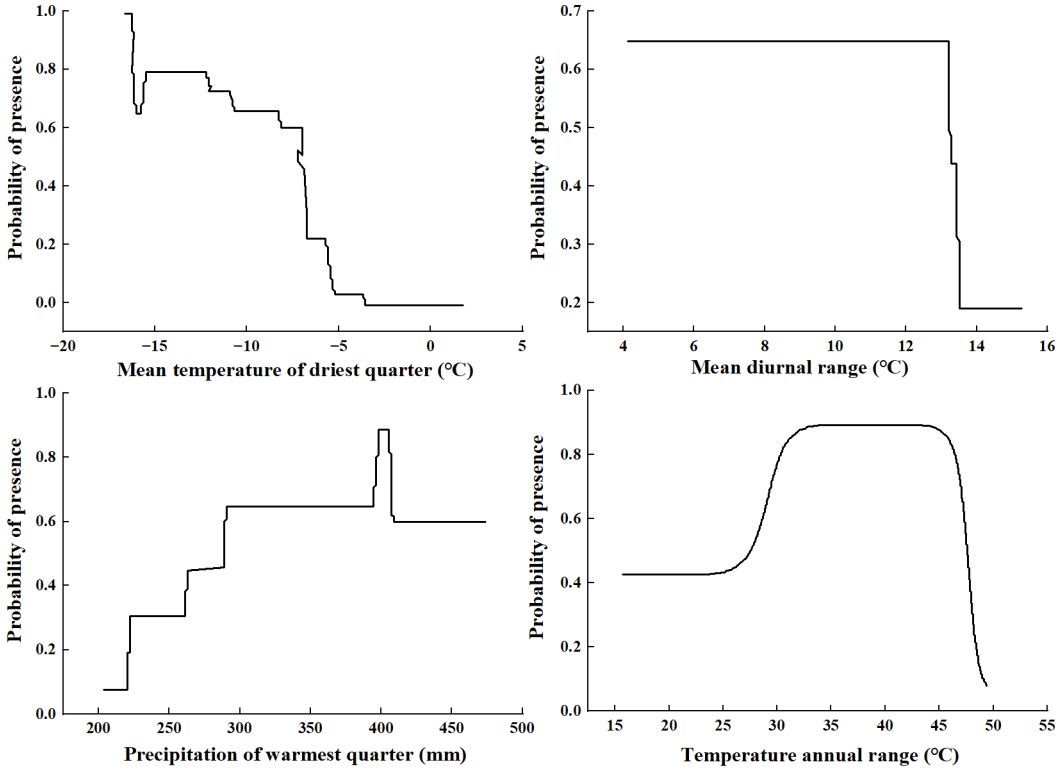

Figure 3. Response curve analysis on dominant environmental variables for *L. principis-rupprechtii*.

3.3. Current Suitable Distribution

The suitable distribution map of larch under the current climatic conditions was obtained based on the prediction results of the EM (Figure 4). The results showed that the suitable distribution areas for larch were mainly distributed in Yan Mountain, Xiaowutai Mountain, and Bashang Plateau of Hebei Province, and in Lvliang Mountain, Wutai Mountain, and Heng Mountain of Shanxi Province. The area proportions of highly suitable, moderately suitable, lowly suitable area, and unsuitable habitats were 12.38%, 12.67%, 12.01%, and 62.94%, respectively (Table 4).

Table 4. Different classes of suitable area for *L. principis-rupprechtii* under current and future climate scenarios.

Year	Scenarios	Area (km^2) (Percentage%)			
		Unsuitable	Lowly Suitable	Moderately Suitable	Highly Suitable
Current	-	217,466.11 (62.94)	41,490.91 (12.01)	43,775.43 (12.67)	42,767.55 (12.38)
2030s	SSP1-2.6	251,465.14 (72.78)	31,949.68 (9.25)	29,295.60 (8.48)	32,789.58 (9.49)
	SSP2-4.5	267,255.20 (77.35)	23,063.57 (6.68)	27,431.03 (7.94)	27,750.19 (8.03)
	SSP5-8.5	244,645.18 (70.81)	43,288.29 (12.53)	29,480.38 (8.53)	28,086.15 (8.13)
2050s	SSP1-2.6	239,840.97 (69.42)	50,343.42 (14.57)	27,750.19 (8.03)	27,565.42 (7.98)
	SSP2-4.5	267,759.14 (77.50)	32,184.85 (9.32)	23,046.77 (6.67)	22,509.24 (6.51)
	SSP5-8.5	268,565.44 (77.73)	31,176.97 (9.02)	22,173.28 (6.42)	23,584.31 (6.83)
2090s	SSP1-2.6	251,414.75 (72.77)	40,768.60 (11.80)	26,943.89 (7.80)	26,372.76 (7.63)
	SSP2-4.5	291,595.42 (84.40)	23,365.93 (6.76)	15,151.74 (4.39)	15,386.91 (4.45)
	SSP5-8.5	312,962.39 (90.58)	14,966.96 (4.33)	8835.72 (2.56)	8734.93 (2.53)

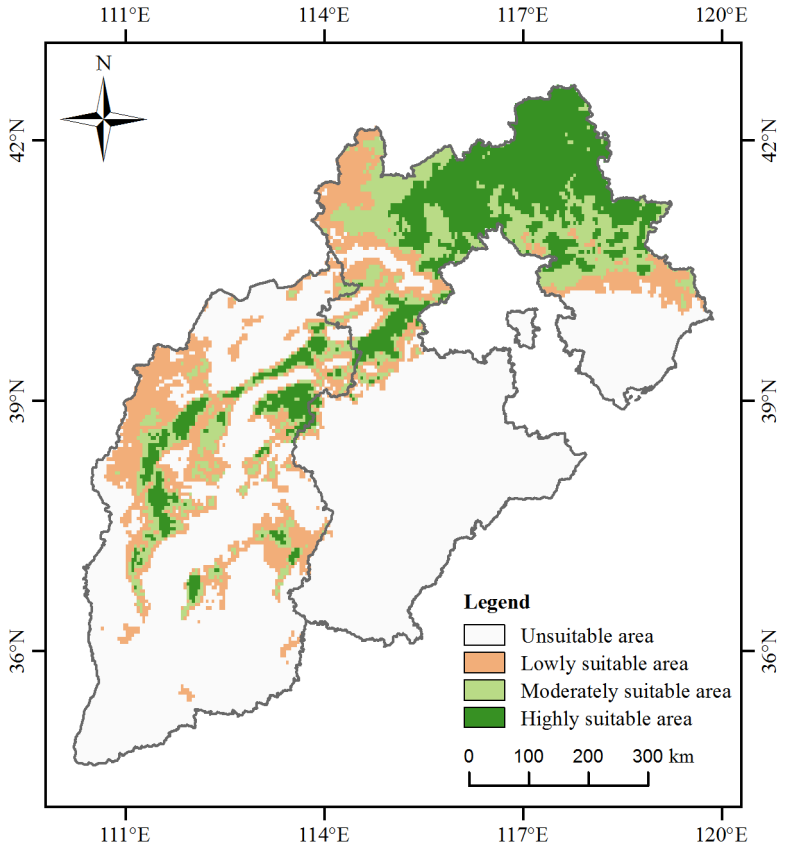

Figure 4. Current suitable distribution area of *L. principis-rupprechtii*.

3.4. Future Suitable Distribution

The suitable distribution areas of larch varied greatly under different climate scenarios in the future (Table 4 and Figure 5). Under the SSP1-2.6 climate scenario, the moderately and highly suitable distribution areas showed a decreasing trend by the 2050s but showed an increasing trend by the 2090s. However, under the SSP2-4.5 and SSP5-8.5 climate scenarios, the moderately and highly suitable areas showed a significantly decreasing trend by the 2090s, especially under the SSP5-8.5 climate scenario. Based on the SSP5-8.5 climate scenario, the total unsuitable areas increased by 90.58% in 2090, whereas the moderately and highly suitable areas decreased by 2.56% and 2.53%, respectively (Table 4).

In the SSP1-2.6 climate scenario, the distribution areas did not change much in different periods (Figure 5). Under the SSP2-4.5 climate scenario, the suitable distribution areas tended to migrate to high latitudes, while the suitable distribution areas of low latitudes continued to shrink, even lost by the end of this century. Under the SSP5-8.5 climate scenario, larch distribution showed extreme changes, and all the suitable distribution areas except Bashang distributed in Zhangjiakou and Chengde regions in the low latitudes were lost by the end of this century.

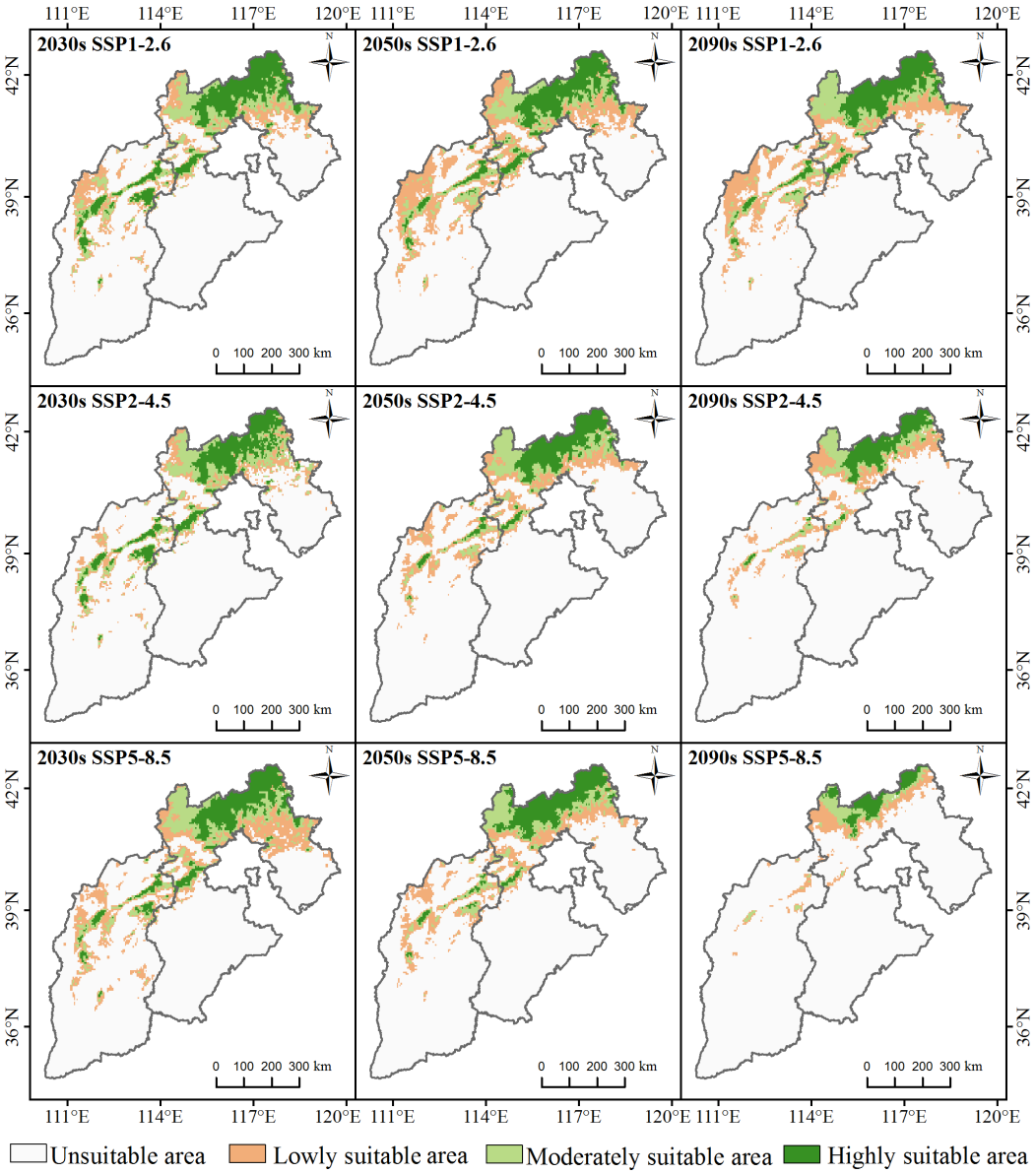

Figure 5. Potential spatial distribution of *L. principis-rupprechtii* under different climate change scenarios in 2030s–2090s based on the ensemble model.

Under the three climate scenarios SSP1-2.6, SSP2-4.5, and SSP5-8.5, The area of unsuitable areas increased rapidly before 2030, while decreased under SSP1-2.6 and SSP2-4.5 between the 2030s and 2050s. However, there was a significant increase in the area of unsuitable areas under different climatic scenarios after the 2050s. The area changes of lowly suitable areas showed a fluctuating state, whereas the area of moderately and highly suitable areas showed a downward trend under three climatic scenarios. From SSP1-2.6 to SSP5-8.5 climate scenarios, the area of moderately and highly suitable areas of *L. principis-rupprechtii* decreased more sharply (Figure 6).

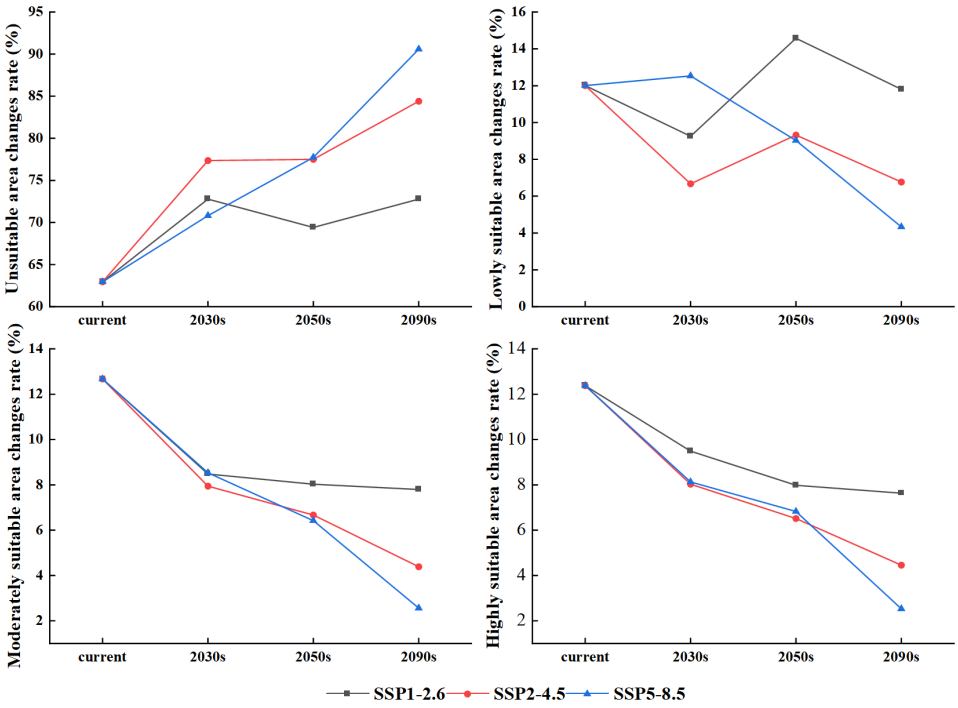

Figure 6. Change in the area of the different suitable areas of *L. principis-rupprechtii* in future climate scenarios.

3.5. The Change of Suitable Distribution Pattern in the Future

Overlay analysis indicated that the increased potential suitable areas were smaller than the degraded potential suitable areas, and there was a peak in the increased potential suitable areas in the 2050s (Figure 7 and Table 5). The increased potential suitable areas were mainly concentrated in Guancen Mountain and Hongtao Mountain in the northwest of Shanxi Province and Daqing Mountain in the northwest of Hebei Province. Under the SSP1-2.6 climate scenario, the change of unsuitable and degraded suitable areas of *L. principis-rupprechtii* would be significant in the 2030s, but not in the 2050s and 2090s. Under the SSP2-4.5 climate scenario, except for increased potential suitable and unsuitable areas, the area of degraded potential suitable areas increased significantly. Under the SSP5-8.5 climate scenario, the degraded suitable areas increased sharply, accounting for 30.60% of the total area until the 2090s.

Table 5. Spatial variation in suitable distribution areas of *L. principis-rupprechtii* in different periods.

Scenarios	Year	Area (km^2) (Percentage is Shown in Brackets)			
		Unsuitable Areas	Unchangeable Potential Suitable Areas	Degraded Potential Suitable Areas	Increased Potential Suitable Areas
SSP1-2.6	2030s	206,749.03 (59.84)	93,463.73 (27.05)	44,716.11 (12.94)	571.13 (0.17)
	2050s	201,810.43 (58.41)	100,149.31 (28.99)	38,030.53 (11.01)	5509.72 (1.59)
	2090s	203,322.25 (58.85)	90,087.34 (26.07)	48,092.50 (13.92)	3997.91 (1.16)
SSP2-4.5	2030s	207,320.16 (60.01)	78,244.80 (22.65)	59,935.04 (17.35)	0.00 (0.00)
	2050s	205,338.00 (59.43)	75,758.70 (21.93)	62,421.14 (18.07)	1982.16 (0.57)
	2090s	207,269.76 (59.99)	53,854.19 (15.59)	84,325.65 (24.41)	50.39 (0.01)
SSP5-8.5	2030s	206,967.40 (59.90)	100,502.07 (29.09)	37,677.78 (10.91)	352.76 (0.10)
	2050s	206,043.51 (59.64)	75,657.92 (21.90)	62,521.93 (18.10)	1276.64 (0.37)
	2090s	207,252.97 (59.99)	32,470.42 (9.40)	105,709.43 (30.60)	67.19 (0.02)

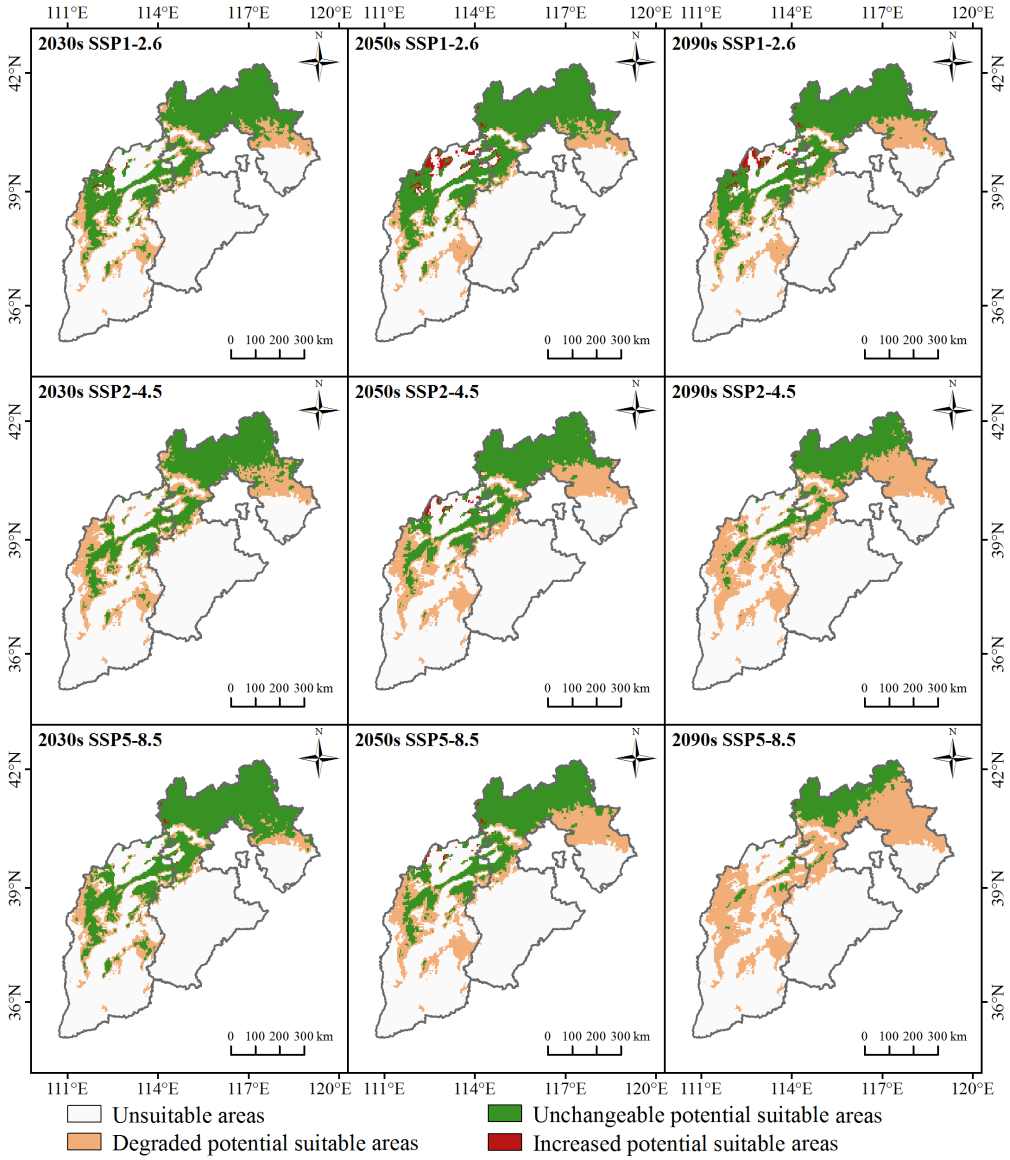

Figure 7. The spatial pattern of suitable areas for *L. principis-rupprechtii* in different periods.

3.6. Centroid Migration

There were some differences in centroid and migration distance among different suitable areas under different climatic scenarios (Figure 8, Table 6). At present, the centroids of lowly, moderately, and highly suitable areas of *L. principis-rupprechtii* shifted from southwest to northeast. In the future different climate scenarios, the centroids of lowly, moderately, and highly suitable areas of *L. principis-rupprechtii* would migrate towards north. With increasing climate scenario concentrations, the migration distance increased significantly. Under the SSP5-8.5 climate scenario, the migration distances of highly, moderately, and lowly suitable areas were 232.60 km, 206.75 km, and 163.43 km, respectively.

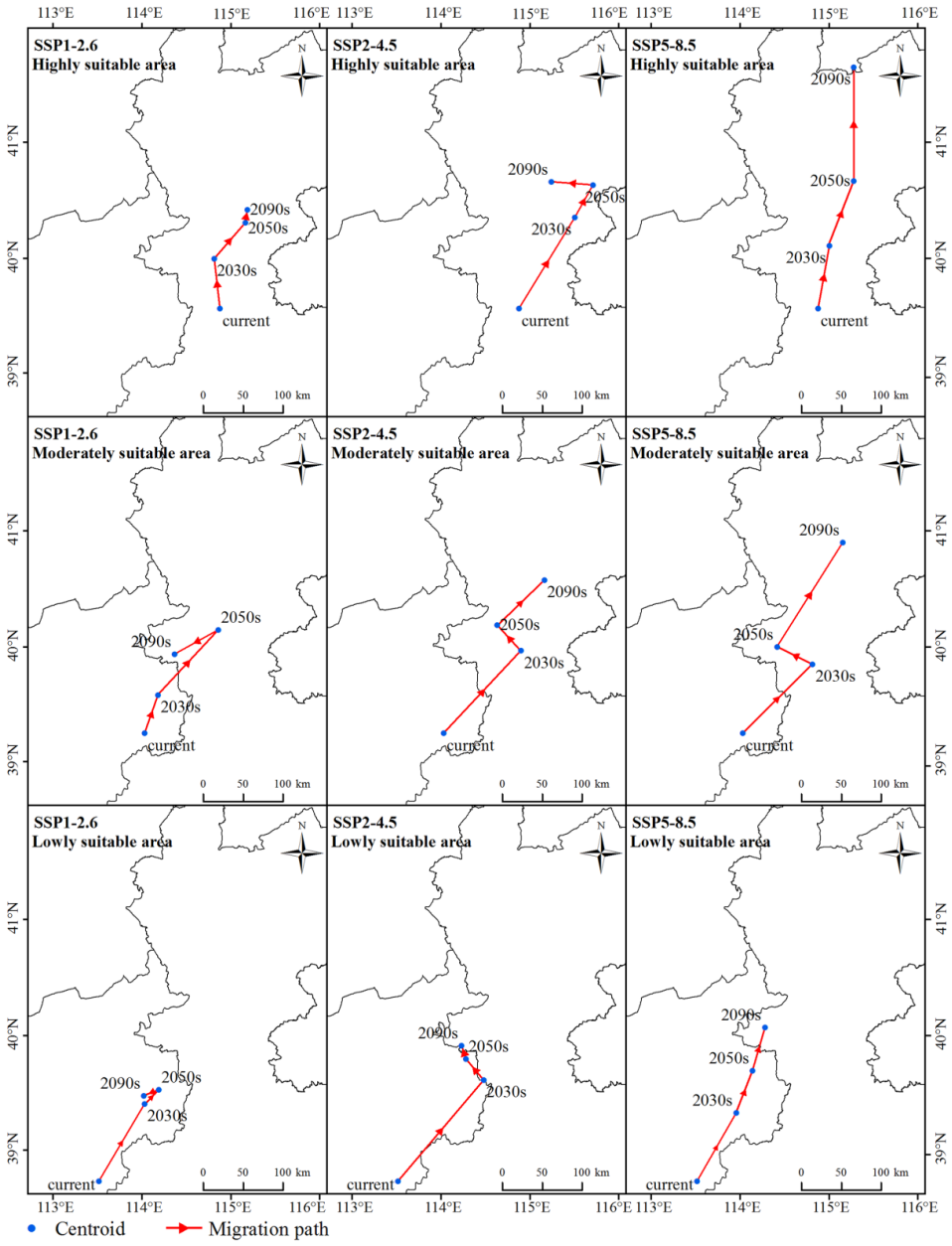

Figure 8. Centroid shifts under current and future climate scenarios for *L. principis-rupprechtii*.

Table 6. Centroid shift distances under current and future climate scenarios for *L. principis-rupprechtii*.

Scenarios	Year	Highly Suitable			Moderately Suitable			Lowly Suitable		
		Longitude (°)	Latitude (°)	Migration Distance (km)	Longitude (°)	Latitude (°)	Migration Distance (km)	Longitude (°)	Latitude (°)	Migration Distance (km)
SSP1-2.6	Current	114.87	39.56		114.02	39.25		113.51	38.72	
	2030s	114.81	40.00	48.40	114.18	39.58	39.09	114.02	39.41	87.83
	2050s	115.16	40.31	86.58	114.85	40.15	122.62	114.18	39.53	106.73
	2090s	115.18	40.42	98.81	114.36	39.94	81.75	114.02	39.48	94.38
SSP2-4.5	2030s	115.50	40.35	103.07	114.90	39.97	109.44	114.48	39.61	129.43
	2050s	115.70	40.63	138.27	114.63	40.19	116.49	114.28	39.80	136.11
	2090s	115.24	40.66	125.62	115.16	40.58	176.60	114.23	39.91	145.88
SSP5-8.5	2030s	115.00	40.11	61.59	114.81	39.85	94.91	113.95	39.33	76.95
	2050s	115.27	40.67	127.26	114.41	40.005	89.79	114.13	39.69	120.45
	2090s	115.28	41.63	232.60	115.15	40.90	206.75	114.27	40.07	163.43

4. Discussion

4.1. Ensemble Model Evaluation

At present, the research on the suitable distribution of *L. principis-rupprechtii* is mainly focused on the single species distribution model [47,62]. Due to the different algorithms of different models and different ways of dealing with data, there are some differences in the importance of environmental factors, model fitting evaluation, and suitable distribution [63]. For example, Liu et al. [62] found that the dominant factors affecting the distribution of *L. principis-rupprechtii* were the highest temperature of the hottest month, the annual temperature difference, and seasonal temperature variation. However, Lv et al. [47] thought that larch's distribution was mainly affected by the accumulative temperature below 0 °C and the mean precipitation of wet quarter. The uncertainty of a single distribution model can be reduced to some extent by building an EM [31,64]. The "Biomod2" software package can not only predict the current distribution of *L. principis-rupprechtii* in an ensemble way but also predict the potential distribution area under future climate scenarios [35,65]. In this study, based on the "Biomod2" software package, 10 single species distribution models and EM were constructed using the latest CMIP6 climate data, and the results were evaluated by KAPPA, ROC, and TSS. According to the evaluation metrics, the six single species distribution models of FDA, GBM, RF, MAXENT, GLM, and MARS performed better, followed by GAM, ANN, and CTA models, while the SRE model performed the worst. This is consistent with other results using multiple models to predict species distribution, which shows that the simulation effect of RF is better, while the performance of SRE is the worst [2,32,66]. Some studies have shown that there is some uncertainty in using ROC alone to evaluate the model [67]. Therefore, we select the results of a single model with ROC > 0.9 and TSS > 0.7 to construct the EM. The results show that the three indicators of the EM have been significantly improved, in which TSS and ROC have reached an excellent level (TSS = 0.81, ROC = 0.95), KAPPA value has reached a better degree (KAPPA = 0.65). Through the model evaluation, it can be found that the EM was better than the single species distribution model.

4.2. Dominant Climatic Factor

The analysis of the relative importance of climate factors showed that the mean temperature of driest quarter (BIO9) and the mean diurnal range (BIO2) had a significant influence on the suitable distribution of *L. principis-rupprechtii*, with a total relative importance of 64.52%, followed by the precipitation of warmest quarter (BIO18) and temperature annual range (BIO7), with a total relative importance of 16.73%. Other climatic factors had no significant effect on larch's suitable distribution (Table 3). The results showed that temperature was the key factor affecting the suitable distribution of *L. principis-rupprechtii*, which was similar to that of Liu [64] and Liu et al. [62].

The response curve analysis indicated that the suitable ranges were −16.4 to −5.7 °C for BIO9 and the presence probability decreased with increasing temperature. BIO9 is the most important climatic factor to limit the growth of *L. olgensis* [22] and to influence the distribution of *Larix chinensis* [1] and *Larix gmelinii* [68]. BIO9 may affect the respiration process of larch in winter. The low temperature reduces the activity of enzymes and limits the decomposition rate of organic matter, thus storing more assimilated substances for the growth of larch. Some studies have also shown that there is a close relationship between winter temperature and plant distribution [69]. The cold tolerance of larch is the result of long-term adaptation to low temperature in winter [70,71]. It is difficult for larch to adapt to the rapid warming of the climate. The mean diurnal range of *L. principis-rupprechtii* was less than 13.5 °C. BIO2 reflects the change in temperature during the day. Photosynthesis and respiration of plants during the day contribute to the accumulation of nutrients [72,73]. Global climate change shows that the temperature rises faster during the night than during the day [74]. This change is not conducive to the accumulation of plant nutrients. The suitable ranges were 24.7 to 48.4 °C for BIO7. Some studies have also shown that BIO7 influences the distribution of coniferous forests [20] and *L. gmelinii*

in China [68]. The suitable ranges were 222.2 to 409 mm for BIO18, and the presence probability of larch increased with increasing precipitation. When the precipitation reached 409 mm, precipitation was no longer the main factor limiting larch distribution. This was consistent with the characteristics of the temperate monsoon climate in the study area. In the study area, the average annual precipitation ranges from 300 to 800 mm, and the precipitation is mainly concentrated in the warmest season [48,49]. Summer is the main growing season for *L. principis-rupprechtii*. Sufficient precipitation in summer can provide sufficient water for the physiological process and growth of trees [39].

4.3. Suitable Distribution Pattern

The study indicated that climate change had a significant impact on the larch's distribution. Currently, it was mainly distributed in the Bashang Plateau, Yan Mountain, Taihang Mountain, Heng Mountain, Wutai Mountain, and Lvliang Mountain. Our result was consistent with the actual distribution [50,75]. The suitable distribution areas would shrink and migrate to varying degrees under different climatic scenarios in the future, which was consistent with the results of other studies [1,41,43]. The results showed that the distribution of *L. principis-rupprechtii* was sensitive to climate change. The contraction degree under SSP1-2.6 was much lower than that under SSP5-8.5. The suitable distribution areas under different climate scenarios showed a sharp contraction in 2030, then shrank slowly. The reason for this contraction may be that *L. principis-rupprechtii* has a long growth cycle and slow migration, so it is difficult to adapt to rapidly changing climatic conditions [8]. On the other hand, it may be that other tree species invade its distribution areas under the condition of global warming [76].

With the increase in climate scenario concentrations, the more the loss of potential suitable areas, the smaller the increased potential suitable areas. This result may be due to the slow migration of *L. principis-rupprechtii* [8]. However, different climate scenarios showed consistency: increased potential suitable areas were mainly distributed in the northwest of the study area, and the degraded potential suitable areas were mainly located in low latitudes. The topography of the study area is high in the northwest and low in the southeast, which shows that *L. principis-rupprechtii* has a trend of migration to high altitudes. This was consistent with the results of Lv et al. [47]. A study has also shown that future climate change promotes the growth of high-altitude larch and inhibits the growth of low-altitude larch [77]. Under different climate scenarios in the future, the area of degraded potential suitable areas of *L. principis-rupprechtii* was much larger than that of increased potential suitable areas, which was consistent with the results of Zhao et al. [18]. Analyzing distribution pattern changes is helpful for understanding how *L. principis-rupprechtii* might respond to future climates.

4.4. Centroid Migration

Based on the analysis of the centroid and migration distance of different suitable areas, the results showed that the centroids of lowly, moderately, and highly suitable areas of *L. principis-rupprechtii* shifted from southwest to northeast under the current climatic conditions. Under different climatic scenarios in the future, the different suitable distribution areas, except for highly suitable areas, in which centroids showed a northwestward migration in the SSP1-2.6 climate scenario until 2030, generally showed a trend of migration towards the northeast. This was consistent with the migration results of larch [41,43,78]. Our research indicated the migration distance under SSP5-8.5 was about twice as much as that under SSP1-2.6 at the end of this century. Zhao et al. [1] also showed that the degraded area of *L. chinensis* in high concentration climate scenarios was twice as much as that in low concentration climate scenarios. Centroid migration analysis can provide further interpretation of the sensitivity of *L. principis-rupprechtii* to climate change [40].

5. Conclusions

Based on ten single species distribution models, the EM was constructed to predict the suitable distribution of *L. principis-rupprechtii*. The evaluation metrics of ROC, TSS, and KAPPA were significantly improved, indicating the predictive results of the EM were accurate and reliable. Climate factors, including the mean temperature of driest quarter, the mean diurnal range, the precipitation of warmest quarter, and temperature annual range, were the main determinants shaping the distribution of *L. principis-rupprechtii*. Under future climate scenarios, the suitable areas of *L. principis-rupprechtii* would shrink and migrate to high latitudes. From SSP1-2.6 to SSP5-8.5 climate scenarios, the area of moderately and highly suitable areas of *L. principis-rupprechtii* decreased more sharply. Our study further proved that larch's distribution was sensitive to climate change. This work provides a feasible approach to understanding the possible impacts of climate change on *L. principis-rupprechtii*. Our study will be helpful for the sustainable management of *L. principis-rupprechtii* forests.

Author Contributions: Conceptualization, R.C. and Z.Z.; methodology, software, visualization, R.C. and X.W.; investigation, data curation, Z.Z., Z.G., J.Z. (Jing Zhang); writing—original draft preparation, R.C. and J.Z. (Jinman Zhao); writing—review and editing, Z.Z. All authors have read and agreed to the published version of the manuscript.

Funding: This research was funded by National Natural Science Foundation of China, grant number 32071759, the Natural Science Foundation of Hebei Province, China, grant number C2020204026, and the Hebei Province Key R & D Program of China, grant number 22326803D.

Institutional Review Board Statement: Not applicable.

Informed Consent Statement: Not applicable.

Data Availability Statement: The data presented in this study are available on request from the corresponding author.

Acknowledgments: We thank our graduate students and many local staff, who have conducted the field investigation in the study area. Special thanks to the Chinese Virtual Herbarium, the National Specimen Information Infrastructure and WorldClim for their available data in making this simulation possible.

Conflicts of Interest: The authors declare no conflict of interest.

References

1. Zhao, X.; Meng, H.; Wang, W.; Yan, B. Prediction of the Distribution of Alpine Tree Species Under Climate Change Scenarios: Larix chinensisin Taibai Mountain (China). *Pol. J. Ecol.* **2016**, *64*, 200–212. [CrossRef]
2. Xu, Y.; Huang, Y.; Zhao, H.; Yang, M.; Zhuang, Y.; Ye, X. Modelling the Effects of Climate Change on the Distribution of Endangered *Cypripedium japonicum* in China. *Forests* **2021**, *12*, 429. [CrossRef]
3. Subba, B.; Sen, S.; Ravikanth, G.; Nobis, M.P. Direct modelling of limited migration improves projected distributions of Himalayan amphibians under climate change. *Biol. Conserv.* **2018**, *227*, 352–360. [CrossRef]
4. Friedlingstein, P.; Houghton, A.R.; Marland, G.; Hackler, J.; Boden, A.T.; Conway, J.T.; Canadell, G.J.; Raupach, R.M.; Ciais, P.; Quéré, L.C. Update on CO_2 emissions. *Nat. Geosci.* **2010**, *3*, 811–812. [CrossRef]
5. Peters, R.L.; Klesse, S.; Fonti, P.; Frank, D. Contribution of climate vs. larch budmoth outbreaks in regulating biomass accumulation in high-elevation forests. *For. Ecol. Manag.* **2017**, *401*, 147–158. [CrossRef]
6. Wang, T.; Wang, G.; Innes, J.; Nitschke, C.; Kang, H. Climatic niche models and their consensus projections for future climates for four major forest tree species in the Asia–Pacific region. *For. Ecol. Manag.* **2016**, *360*, 357–366. [CrossRef]
7. Dyderski, M.K.; Paź, S.; Frelich, L.E.; Jagodziński, A.M. How much does climate change threaten European forest tree species distributions? *Glob. Chang. Biol.* **2018**, *24*, 1150–1163. [CrossRef]
8. Aitken, S.N.; Yeaman, S.; Holliday, J.A.; Wang, T.; Curtis-McLane, S. Adaptation, migration or extirpation: Climate change outcomes for tree populations. *Evol. Appl.* **2008**, *1*, 95–111. [CrossRef]
9. IPCC. Summary for Policymakers. In *Climate Change 2021: The Physical Science Basis. Contribution of Working Group I to the Sixth Assessment Report of the Intergovernmental Panel on Climate Change*; Intergovernmental Panel on Climate Change: Cambridge, UK; New York, NY, USA, 2021.
10. Stevens, B.S.; Conway, C.J. Predictive multi-scale occupancy models at range-wide extents: Effects of habitat and human disturbance on distributions of wetland birds. *Divers. Distrib.* **2019**, *26*, 34–48. [CrossRef]

11. Guisan, A.; Tingley, R.; Baumgartner, J.B.; Naujokaitis-Lewis, I.; Sutcliffe, P.R.; Tulloch, A.I.T.; Regan, T.J.; Brotons, L.; Mcdonald-Madden, E.; Mantyka-Pringle, C.; et al. Predicting species distributions for conservation decisions. *Ecol. Lett.* **2013**, *16*, 1424–1435. [CrossRef]
12. Poulter, B.; Pederson, N.; Liu, H.; Zhu, Z.; D'Arrigo, R.; Ciais, P.; Davi, N.; Frank, D.; Leland, C.; Myneni, R.; et al. Recent trends in Inner Asian forest dynamics to temperature and precipitation indicate high sensitivity to climate change. *Agric. For. Meteorol.* **2013**, *178–179*, 31–45. [CrossRef]
13. Shuman, J.K.; Shugart, H.; O'Halloran, T. Sensitivity of Siberian larch forests to climate change. *Glob. Chang. Biol.* **2011**, *17*, 2370–2384. [CrossRef]
14. Piao, S.L.; Ciais, P.; Huang, Y.; Shen, Z.H.; Peng, S.S.; Li, J.S.; Zhou, L.P.; Liu, H.Y.; Ma, Y.C.; Ding, Y.H.; et al. The impacts of climate change on water resources and agriculture in China. *Nature* **2010**, *467*, 43–51. [CrossRef] [PubMed]
15. Zhou, G.; Li, L.; Wu, A. Effect of drought on forest ecosystem under warming climate. *J. Nanjing Univ. Inf. Sci. Technol.* **2020**, *12*, 81–88. [CrossRef]
16. Allen, C.D.; Macalady, A.K.; Chenchouni, H.; Bachelet, D.; McDowell, N.; Vennetier, M.; Kitzberger, T.; Rigling, A.; Breshears, D.D.; Hogg, E.H.; et al. A global overview of drought and heat-induced tree mortality reveals emerging climate change risks for forests. *For. Ecol. Manag.* **2010**, *259*, 660–684. [CrossRef]
17. Feeley, K.J.; Bravo-Avila, C.; Fadrique, B.; Perez, T.M.; Zuleta, D. Publisher Correction: Climate-driven changes in the composition of New World plant communities. *Nat. Clim. Chang.* **2020**, *10*, 1062. [CrossRef]
18. Zhao, Z.; Guo, Y.; Zhu, F.; Jiang, Y. Prediction of the impact of climate change on fast-growing timber trees in China. *For. Ecol. Manag.* **2021**, *501*, 119653. [CrossRef]
19. Bertrand, R.; Lenoir, J.; Piedallu, C.; Riofrío-Dillon, G.; De Ruffray, P.; Vidal, C.; Pierrat, J.-C.; Gégout, J.-C. Changes in plant community composition lag behind climate warming in lowland forests. *Nature* **2011**, *479*, 517–520. [CrossRef]
20. Dakhil, M.; Xiong, Q.; Farahat, E.A.; Zhang, L.; Pan, K.; Pandey, B.; Olatunji, O.A.; Tariq, A.; Wu, X.; Zhang, A.; et al. Past and future climatic indicators for distribution patterns and conservation planning of temperate coniferous forests in southwestern China. *Ecol. Indic.* **2019**, *107*, 105559. [CrossRef]
21. Hagerman, S.M.; Pelai, R. Responding to climate change in forest management: Two decades of recommendations. *Front. Ecol. Environ.* **2018**, *16*, 579–587. [CrossRef]
22. Lei, X.; Yu, L.; Hong, L. Climate-sensitive integrated stand growth model (CS-ISGM) of Changbai larch (*Larix olgensis*) plantations. *For. Ecol. Manag.* **2016**, *376*, 265–275. [CrossRef]
23. Guisan, A.; Graham, C.H.; Elith, J.; Huettmann, F.; The NCEAS Species Distribution Modelling Group. Sensitivity of predictive species distribution models to change in grain size. *Divers. Distrib.* **2007**, *13*, 332–340. [CrossRef]
24. Barrett, M.A.; Brown, J.L.; Junge, R.E.; Yoder, A.D. Climate change, predictive modeling and lemur health: Assessing impacts of changing climate on health and conservation in Madagascar. *Biol. Conserv.* **2013**, *157*, 409–422. [CrossRef]
25. Wang, S.; Xu, X.; Shrestha, N.; Zimmermann, N.; Tang, Z.; Wang, Z. Response of spatial vegetation distribution in China to climate changes since the Last Glacial Maximum (LGM). *PLoS ONE* **2017**, *12*, e0175742. [CrossRef]
26. Liu, X.-T.; Yuan, Q.; Ni, J. Research advances in modelling plant species distribution in China. *Chin. J. Plant Ecol.* **2019**, *43*, 273–283. [CrossRef]
27. Rathore, P.; Roy, A.; Karnatak, H. Modelling the vulnerability of Taxus wallichiana to climate change scenarios in South East Asia. *Ecol. Indic.* **2019**, *102*, 199–207. [CrossRef]
28. Segurado, P.; Araújo, M.B. An evaluation of methods for modelling species distributions. *J. Biogeogr.* **2004**, *31*, 1555–1568. [CrossRef]
29. Lopatin, J.; Dolos, K.; Hernández, H.; Galleguillos, M.; Fassnacht, F. Comparing Generalized Linear Models and random forest to model vascular plant species richness using LiDAR data in a natural forest in central Chile. *Remote Sens. Environ.* **2015**, *173*, 200–210. [CrossRef]
30. Phillips, S.J.; Anderson, R.P.; Schapire, R.E. Maximum entropy modeling of species geographic distributions. *Ecol. Model.* **2006**, *190*, 231–259. [CrossRef]
31. Pearson, R.G.; Thuiller, W.; Araújo, M.B.; Martínez-Meyer, E.; Brotons, L.; McClean, C.; Miles, L.; Segurado, P.; Dawson, T.; Lees, D.C. Model-based uncertainty in species range prediction. *J. Biogeogr.* **2006**, *33*, 1704–1711. [CrossRef]
32. Ardestani, E.G.; Rigi, H.; Honarbakhsh, A. Predicting optimal habitats of *Haloxylon persicum* for ecosystem restoration using ensemble ecological niche modeling under climate change in southeast Iran. *Restor. Ecol.* **2021**, *29*, e13492. [CrossRef]
33. Moraitis, M.L.; Valavanis, V.D.; Karakassis, I. Modelling the effects of climate change on the distribution of benthic indicator species in the Eastern Mediterranean Sea. *Sci. Total Environ.* **2019**, *667*, 16–24. [CrossRef] [PubMed]
34. Thuiller, W. BIOMOD—Optimizing predictions of species distributions and projecting potential future shifts under global change. *Glob. Chang. Biol.* **2003**, *9*, 1353–1362. [CrossRef]
35. Ray, D.; Marchi, M.; Rattey, A.; Broome, A. A multi-data ensemble approach for predicting woodland type distribution: Oak woodland in Britain. *Ecol. Evol.* **2021**, *11*, 9423–9434. [CrossRef]
36. Dakhil, M.A.; Halmy, M.W.A.; Liao, Z.; Pandey, B.; Zhang, L.; Pan, K.; Sun, X.; Wu, X.; Eid, E.M.; El-Barougy, R.F. Potential risks to endemic conifer montane forests under climate change: Integrative approach for conservation prioritization in southwestern China. *Landsc. Ecol.* **2021**, *36*, 3137–3151. [CrossRef]

37. Mateo, R.G.; de la Estrella, M.; Felicísimo, Á.M.; Muñoz, J.; Guisan, A. A new spin on a compositionalist predictive modelling framework for conservation planning: A tropical case study in Ecuador. *Biol. Conserv.* **2013**, *160*, 150–161. [CrossRef]
38. Zhou, X.; Wang, X.; Han, S.; Zou, C. The effect of giobal climate change on the dynamics of Betula ermanii-Tundra ecotone in the changbai mountains. *Earth Sci. Front.* **2002**, *9*, 227–231.
39. Fu, L.; Sun, W.; Wang, G. A climate-sensitive aboveground biomass model for three larch species in northeastern and northern China. *Trees* **2016**, *31*, 557–573. [CrossRef]
40. Sun, Y.; Wang, L. Global research progresses in dendroclimatology of *Larix Miller*. *Prog. Geogr.* **2013**, *32*, 1760–1770. [CrossRef]
41. Wu, C.; Chen, D.; Shen, J.; Sun, X.; Zhang, S. Estimating the distribution and productivity characters of *Larix kaempferi* in response to climate change. *J. Environ. Manag.* **2020**, *280*, 111633. [CrossRef]
42. Leng, W.; He, H.; Bu, R.; Hu, Y.; Wang, X. Potential impact of climate change on distribution of *Larix* genus of northeastern China. *For. Ecol. Manag.* **2008**, *254*, 420–428. [CrossRef]
43. Leng, W.; He, H.; Bu, R.; Hu, Y. Sensitivity analysis of the impacts of climate change on potential distribution of three Larch (*Larix*) species in Northeastern China. *J. Plant Ecol.* **2007**, *31*, 825–833.
44. Zhao, K.; Wang, L.; Wang, L.; Jia, Z.; Ma, l. Stock volume and productivity of *Larix principis-rupprechtiiin* northern and northwestern China. *J. Beijing For. Univ.* **2015**, *37*, 24–31. [CrossRef]
45. Ye, S.; Dong, G.; Shao, C.; Liu, Y. Selection of tree species in accurate quality improvement of *Larix principis-rupprechtii* plantation. *Bull. Soil. Water Conserv.* **2018**, *38*, 162–168. [CrossRef]
46. Mu, X.; Wu, Z.; Li, X.; Wang, F.; Bai, X.; Guo, S.; Cheng, R.; Yu, S. Estimation of the potential distribution areas of *Larix principis-rupprechtii* plantation in Chifeng based on MaxEnt model. *J. Arid Land Resour. Environ.* **2021**, *35*, 144–152. [CrossRef]
47. Lv, Z.; Li, W.; Huang, X.; Zhang, Z. Predicting suitable distribution areas of three dominant tree species under climate change scenarios in Hebei Province. *Sci. Silvae Sin.* **2019**, *55*, 13–21. [CrossRef]
48. Gao, Q.; Che, S.; Han, J. Characteristic of climate change in Hebei Province and its influence on phenology. *J. Anhui Agric. Sci.* **2010**, *38*, 18319–18323. [CrossRef]
49. Wang, Y.; Liu, Z. Shanxi forestry climatic resources. *Shanxi For. Sci. Technol.* **2004**, *51*, 37–40.
50. Zheng, W. *Chinese Tree Chronicles*; China Forestry Publishing House: Beijing, China, 1983; Volume 1.
51. Fick, S.E.; Hijmans, R.J. WorldClim 2: New 1-km spatial resolution climate surfaces for global land areas. *Int. J. Climatol.* **2017**, *37*, 4302–4315. [CrossRef]
52. Radosavljevic, A.; Anderson, R.P. Making better Maxent models of species distributions: Complexity, overfitting and evaluation. *J. Biogeogr.* **2013**, *41*, 629–643. [CrossRef]
53. Dang, A.T.; Kumar, L.; Reid, M.; Anh, L.N. Modelling the susceptibility of wetland plant species under climate change in the Mekong Delta, Vietnam. *Ecol. Inform.* **2021**, *64*, 101358. [CrossRef]
54. Jiang, X.-L.; An, M.; Zheng, S.-S.; Deng, M.; Su, Z.-H. Geographical isolation and environmental heterogeneity contribute to the spatial genetic patterns of *Quercus kerrii* (Fagaceae). *Heredity* **2017**, *120*, 219–233. [CrossRef] [PubMed]
55. Thuiller, W. Editorial commentary on 'BIOMOD—Optimizing predictions of species distributions and projecting potential future shifts under global change'. *Glob. Chang. Biol.* **2014**, *20*, 3591–3592. [CrossRef] [PubMed]
56. Thuiller, W.; Lafourcade, B.; Engler, R.; Araújo, M.B. BIOMOD-a platform for ensemble forecasting of species distributions. *Ecography* **2009**, *32*, 369–373. [CrossRef]
57. Uusitalo, R.; Siljander, M.; Culverwell, C.L.; Mutai, N.C.; Forbes, K.M.; Vapalahti, O.; Pellikka, P.K. Predictive mapping of mosquito distribution based on environmental and anthropogenic factors in Taita Hills, Kenya. *Int. J. Appl. Earth Obs. Geoinf. ITC J.* **2018**, *76*, 84–92. [CrossRef]
58. Zhang, L.; Liu, S.; Sun, P.; Wang, T. Partitioning and mapping the sources of variations in the ensemble forecasting of species distribution under climate change: A case study of *Pinus tabulaeformis*. *Acta Ecol. Sin.* **2011**, *31*, 5749–5761.
59. Lasram, F.B.R.; Guilhaumon, F.; Albouy, C.; Somot, S.; Thuiller, W.; Mouillot, D. The Mediterranean Sea as a 'cul-de-sac' for endemic fishes facing climate change. *Glob. Chang. Biol.* **2010**, *16*, 3233–3245. [CrossRef]
60. Allouche, O.; Tsoar, A.; Kadmon, R. Assessing the accuracy of species distribution models: Prevalence, kappa and the true skill statistic (TSS). *J. Appl. Ecol.* **2006**, *43*, 1223–1232. [CrossRef]
61. Brown, J.L.; Bennett, J.R.; French, C.M. SDMtoolbox 2.0: The next generation Python-based GIS toolkit for landscape genetic, biogeographic and species distribution model analyses. *PeerJ* **2017**, *5*, e4095. [CrossRef]
62. Liu, X.; Han, W.; Gao, R.; Jia, J.; Bai, J.; Xu, J.; Gao, W. Potential impacts of environmental types on geographical distri-bution of *Larix principis-rupprechtii*. *Acta Ecol. Sin.* **2021**, *41*, 1885–1893. [CrossRef]
63. Bi, Y.; Xu, J.; Li, Q.; Guisan, A.; Thuiller, W.; Zimmermann, N.E.; Yang, Y.; Yang, X. Applying BioMod for model-ensemble in species distributions: A case study for *Tsuga chinensisin* China. *Plant Divers. Resour.* **2013**, *35*, 647–655. [CrossRef]
64. Liu, D. *Qunatitative Assessment of Matching Trees to Sites Based on Both Distribution Suitability and Potential Site Productivity*; Chinese Academy of Forestry: Beijing, China, 2018.
65. Pavlović, L.; Stojanovic, D.; MladenoviĆ, E.; Lakićević, M.; Orlović, S. Potential Elevation Shift of the European Beech Stands (*Fagus sylvatica* L.) in Serbia. *Front. Plant Sci.* **2019**, *10*, 849. [CrossRef] [PubMed]
66. Zhao, Z.; Guo, Y.; Wei, H.; Ran, Q.; Liu, J.; Zhang, Q.; Gu, W. Potential distribution of *Notopterygium incisum* Ting ex H. T. Chang and its predicted responses to climate change based on a comprehensive habitat suitability model. *Ecol. Evol.* **2020**, *10*, 3004–3016. [CrossRef] [PubMed]

67. Mainali, K.P.; Warren, D.; Dhileepan, K.; Mc Connachie, A.; Strathie, L.; Hassan, G.; Karki, D.; Shrestha, B.B.; Parmesan, C. Projecting future expansion of invasive species: Comparing and improving methodologies for species distribution modeling. *Glob. Chang. Biol.* **2015**, *21*, 4464–4480. [CrossRef]
68. Yang, Z.; Zhou, G.; Yin, X.; Jia, B. Geographic distribution of *Larix gmelinii* natural forest in China and its climatic suitability. *Chin. J. Ecol.* **2014**, *33*, 1429–1436. [CrossRef]
69. Sakai, A. Comparative study on freezing resistance of conifers with special reference to cold adaptation and its evolutive aspects. *Can. J. Bot.* **1983**, *61*, 2323–2332. [CrossRef]
70. Sakai, A.; Weiser, C.J. Freezing Resistance of Trees in North America with Reference to Tree Regions. *Ecology* **1973**, *54*, 118–126. [CrossRef]
71. Sakai, A.; Wardle, P. Freezing resistance of new zealand trees and shrubs. *N. Z. J. Ecol.* **1978**, *1*, 51–61.
72. Bachman, G.R.; McMahon, M.J. Day and Night Temperature Differential (DIF) or the Absence of Far-red Light Alters Cell Elongation in 'Celebrity White' Petunia. *J. Am. Soc. Hortic. Sci.* **2006**, *131*, 309–312. [CrossRef]
73. Wang, X.; Zhang, W.; Zhao, X.; Zhu, H.; Ma, L.; Qian, Z.; Zhang, Z. Modeling the Potential Distribution of Three Taxa of *Akebia* Decne. under Climate Change Scenarios in China. *Forests* **2021**, *12*, 1710. [CrossRef]
74. Wang, J.; Xi, Z.; He, X.; Chen, S.; Rossi, S.; Smith, N.G.; Liu, J.; Chen, L. Contrasting temporal variations in responses of leaf unfolding to daytime and nighttime warming. *Glob. Chang. Biol.* **2021**, *27*, 5084–5093. [CrossRef] [PubMed]
75. Fang, W.; Cai, Q.; Zhu, J.; Ji, C.; Yue, M.; Guo, W.; Zhang, F.; Gao, X.; Tang, Z.; Fang, J. Distribution, community structures and species diversity of larch forests in North China. *Chin. J. Plant Ecol.* **2019**, *43*, 742–752. [CrossRef]
76. Kharuk, V.I.; Ranson, K.J.; Dvinskaya, M. Evidence of Evergreen Conifers Invasion into Larch Dominated Forests During Recent Decades. In *Environmental Change in Siberia*; Springer: Dordrecht, The Netherlands, 2010; pp. 53–65. [CrossRef]
77. Bai, X.; Zhang, X.; Li, J.; Duan, X.; Jin, Y.; Chen, Z. Altitudinal disparity in growth of Dahurian larch *(Larix gmelinii Rupr.)* in response to recent climate change in northeast China. *Sci. Total Environ.* **2019**, *670*, 466–477. [CrossRef] [PubMed]
78. Leng, W.; He, H.S.; Liu, H. Response of larch species to climate changes. *J. Plant Ecol.* **2008**, *1*, 203–205. [CrossRef]